

Tpl2 induces castration resistant prostate cancer progression and metastasis

Hye Won Lee^{1,2,3}, Hyun Jung Cho², Se Jeong Lee^{2,4}, Hye Jin Song^{2,4}, Hee Jin Cho^{1,2}, Min Chul Park⁵, Ho Jun Seol², Jung-Il Lee², Sunghoon Kim⁵, Hyun Moo Lee³, Han Yong Choi³, Do-Hyun Nam^{1,2} and Kyeong Min Joo^{1,4}

¹Samsung Advanced Institute for Health Sciences and Technology (SAIHST), Samsung Medical Center, Sungkyunkwan University School of Medicine, Seoul, South Korea

²Department of Neurosurgery, Samsung Medical Center, Sungkyunkwan University School of Medicine, Seoul, South Korea

³Department of Urology, Samsung Medical Center, Sungkyunkwan University School of Medicine, Seoul, South Korea

⁴Department of Anatomy and Cell Biology, Sungkyunkwan University School of Medicine, Center for Molecular Medicine, Samsung Biomedical Research Institute, Suwon, South Korea

⁵Medicinal Bioconvergence Research Center, College of Pharmacy, Seoul National University, Seoul, South Korea

Progression to metastatic castration resistant prostate cancer (CRPC) is the major lethal pathway of prostate cancer (PC). Herein, we demonstrated that tumor progression locus 2 (Tpl2) kinase is the fundamental molecule provoking progression and metastasis of CRPC. Tpl2 upregulates CXCR4 and focal adhesion kinase (FAK) to activate CXCL12/CXCR4 and FAK/Akt signalling pathway. Consequently, epithelial–mesenchymal transition (EMT) and stemness of androgen depletion independent (ADI) PC cells are induced, which is dependent on the kinase activity of Tpl2. *In vitro*, proliferation, clonogenicity, migration, invasion and chemoresistance of ADI PC cells were enhanced by Tpl2. *In vivo*, Tpl2 overexpression and downregulation showed significant stimulatory and inhibitory effects on tumorigenic and metastatic potential of ADI PC cells, respectively. Moreover, the prognostic effects of Tpl2 and expressional correlation between Tpl2 and EMT-related molecules/CXCR4 were validated in clinical PC databases. Since Tpl2 exerts metastatic progression promoting activities in CRPC, Tpl2 could serve as a novel therapeutic target for metastatic CRPC.

Key words: prostate cancer, castration resistance, tumor progression locus 2, metastasis

Abbreviations: ADI: androgen depletion independent; ccRCC: clear cell renal cell carcinoma; CRPC: castration resistant prostate cancer; CSC: cancer stem cell; CXCR4: chemokine (C-X-C motif) receptor 4; CXCL12: chemokine (C-X-C motif) ligand 12; EMT: epithelial–mesenchymal transition; FAK: Focal adhesion kinase; MSKCC: Memorial Sloan-Kettering Cancer Center; PC: prostate cancer; TCGA: The Cancer Genome Atlas; Tpl2: tumor progression locus 2

Additional Supporting Information may be found in the online version of this article.

Kyeong Min Joo preferred communicator with the Editorial and Production offices

DOI: 10.1002/ijc.29248

History: Received 22 Apr 2014; Accepted 9 Sep 2014; Online 1 Oct 2014

Correspondence to: Do-Hyun Nam, Department of Neurosurgery, Institute for Refractory Cancer Research, Samsung Medical Center, Sungkyunkwan University School of Medicine, 50 Irwon-Dong, Gangnam-Gu, Seoul 135-710, South Korea. Tel.: +82-2-3410-3497; Fax: +82-2-2148-9829; E-mail: nsnam@skku.edu and Correspondence to: Kyeong Min Joo, Department of Anatomy and Cell Biology, Sungkyunkwan University School of Medicine, Samsung Medical Center, 50 Irwon-Dong, Gangnam-Gu, Seoul 135-710, South Korea. Tel.: +82-2-2148-9779; Fax: +82-2-2148-9829; E-mail: kmjoo@skku.edu

Prostate cancer (PC) is the most common cancer and second leading cause of cancer-related deaths in males in the United States.¹ Although androgen depletion therapy is highly effective in suppressing PC growth, persistent androgen ablation often results in the development of metastatic castration resistant prostate cancer (CRPC).² Currently, patients with metastatic CRPC are treated with taxane-based chemotherapeutic drugs. However, the treatment only serves as a palliative, and distant metastasis is the main cause of PC-related death.³ Therefore, the identification of novel therapeutic targets in metastatic CRPC is the most urgent clinical requirement that remains unmet.

Tumors contain a reservoir of cancer stem cells (CSCs) that are responsible for tumor initiation, progression, metastasis and therapeutic resistance.⁴ Since emerging evidence suggests that PC CSCs represent the “bad seeds” of tumor, the molecular mechanisms that maintain PC CSCs could potentially serve as therapeutic targets for metastatic CRPC.^{5,6} Although aldehyde dehydrogenase (ALDH) activity⁷ and expression of CD44⁸ and Bmi-1⁹ have been suggested as specific PC CSC markers, using these markers as therapeutic targets is challenging because the molecules lack specific functional and/or enzymatic activities.

Tumor progression locus 2 [Tpl2/MAP3 kinase 8 (MAP3K8)], a serine/threonine protein kinase, has been suggested to enhance tumor growth and metastatic progression in distinct types of human cancers.^{10–12} Previously, we

What's new?

Prostate cancer turns deadly when it metastasizes and the removal of available androgens – castration -- can no longer hinder it. In this paper, the authors report that the kinase Tpl2 spurs this transition to metastasis. Not only did they find more Tpl2 mRNA in metastatic cells than in non-metastatic, they also showed that Tpl2 upregulates two signaling pathways integral to metastasis. The kinase activity of Tpl2 also support the development of stem cell capabilities in the cancer cells. These results suggest that targeting Tpl2 could impede the spread of prostate cancer.

reported that Tpl2 is a novel oncogene linked to the disease progression and metastasis of clear cell renal cell carcinoma (ccRCC).¹³ Intriguingly, Tpl2 is a key signal transducer of arsenite, which is a critical risk factor of PC.¹⁴ Moreover, a recent study suggested that Tpl2 is a crucial player associated with the progression of PC to the CRPC state.¹⁵ Since Tpl2 expression increases considerably more in metastatic PC than in localized PC cases,¹⁵ Tpl2 may also be associated with the metastatic progression of CRPC.

In this study, we translationally demonstrated a crucial role of Tpl2 in the tumor progression and metastasis of CRPC and, for the first time, investigated underlying molecular mechanisms that enable Tpl2 to function as a metastasis promoting gene in androgen depletion independent (ADI) PC cells.

Material and Methods**PC genomic datasets**

Transcriptome and clinical data of three PC cohorts, the University of Pittsburgh Cancer Institute,¹⁰ the Memorial Sloan-Kettering Cancer Center (MSKCC) and The Cancer Genome Atlas (TCGA), were downloaded from <http://www.ncbi.nlm.nih.gov/geo> (GSE6919), <http://cbio.mskcc.org/prostate-portal/> (GSE21032) and <http://cancergenome.nih.gov/>, respectively.

Cell culture and sublines

Human ADI PC cell lines, 22Rv1, PC3 and DU145, were purchased from American Type Culture Collection. C4-2B cell line, a CRPC-mimicking subline of human LNCaP cell line, was kindly provided by Prof. Jeong (Medical College of Wisconsin). All cell lines were maintained in RPMI-1640 supplemented with 10% fetal bovine serum (FBS) and 1% penicillin/streptomycin (GIBCO). In some experiments using C4-2B cells, charcoal stripped FBS (Life technologies) was alternatively used. PC3 and C4-2B cells that stably express either a nontargeting or Tpl2-targeting shRNA PLKO vector (Prof. Jeong) and 22Rv1 cells that stably express either a pLenti-GIII-CMV empty or Tpl2 vector were established by lentiviral transduction (Invitrogen) and puromycin selection (3 µg/mL, GIBCO).

Reagents

The Tpl2-specific kinase inhibitor (KI) [4-(3-chloro-4-fluorophenylamino)-6-(pyridin-3-yl-methylamino)-3-cyano-1,7-naphthylridine], chemokine (C-X-C motif) receptor 4

(CXCR4) antagonist (AMD3100, Calbiochem), focal adhesion kinase (FAK) inhibitor (PF-573,228), pan-Akt inhibitor (GSK690,693), docetaxel (Selleck Chemicals) and chemokine (C-X-C motif) ligand 12 (CXCL12; PeproTech) were utilized.

Western blotting and quantitative real time-PCR

For WB, cells were lysed in RIPA lysis buffer. Equal amounts of protein were subjected to SDS-polyacrylamide gels electrophoresis and then transferred to PVDF membranes (Whatman). Membranes were blocked in 5% skim milk or bovine serum albumin for 1 hr at room temperature (RT), incubated with indicated primary antibodies overnight and then blotted with the appropriate secondary antibodies. Primary antibodies: Tpl2 (Santa Cruz); FAK, Akt, p-Akt (Thr308, Ser473), ERK, p-ERK, c-Jun N-terminal kinase (JNK) and p-JNK (Cell Signaling); p-FAK (Tyr397, Tyr576), E-cadherin, vimentin, ZEB1, CXCR4, CD44 and Bmi-1 (Abcam); GAPDH (Santa Cruz). For quantitative real time-polymerase chain reaction (qRT-PCR), mRNA was extracted using a RNeasy kit (Qiagen) and then used for subsequent RT using SuperScript III First-Strand Synthesis SuperMix (Invitrogen). The cDNA obtained was used for PCR performed using power SYBR[®] Green PCR Master Mix (Applied Biosystems) and gene-specific primers (Supporting Information Table S1).

Orthotopic PC xenografts

Six to eight-week-old male athymic nude mice were obtained from Orient Bio (Korea). All animal experiments were approved by the Institutional Review Boards of Samsung Medical Center (Seoul, Korea) and conducted in accord with the "National Institute of Health Guide for the Care and Use of Laboratory Animals" (NIH publication No. 80-23, revised in 1996). Two million cells in 40 µL Hank's balanced salt solution were injected into the right prostatic lobe through a midline lower-abdominal incision using a 1-mL syringe with a 27-gauge needle. A well-localized bleb within the injected prostatic lobe was considered as an acceptable injection.

Immunohistochemistry

Endogenous peroxidase activity was blocked by 0.3% hydrogen peroxide. Antigens were retrieved by heating sections in 10 mM sodium citrate (pH 6.0) at 95°C for 30 min. Primary antibodies (4°C, overnight), biotinylated secondary antibodies (1 hr, RT) and then avidin-biotin complex (Vector

Laboratories, 1 hr, RT) were incubated with the sections. Primary antibodies; Tpl2, ZEB1 (Santa Cruz), E-cadherin, vimentin (Dako), CD44, Bmi-1, p-FAK (Y397; Abcam), p-Akt (S473; Cell Signaling) and CXCR4 (Novus).

Proliferation assay

Cells (3×10^3 cells/well in 100 μ L 10% FBS/RPMI) were seeded in 96-well plates. After 1, 24, 48 or 72 hr, cell viability was measured using an EZ-Cytox cell viability assay kit (Daeil Lab) according to the manufacturer's instructions. Alternatively, cells plated were incubated overnight, treated with indicated concentrations of each inhibitor for 72 hr and then analyzed.

Focus forming assay

Three hundred cells per well in 6-well plates were maintained in 10% FBS/RPMI for 2 weeks with or without indicated inhibitors. The number of colonies/well was determined.

Migration/invasion assay

Serum starved cells for 24 hr (1×10^5 cells) were suspended in 300 μ L serum-free RPMI media, added to the upper chamber of modified Boyden chamber (Corning), and then allowed either to migrate through an 8- μ m-pore polycarbonate filter in the migration assay, or to invade through the filter precoated with 100 μ g of Matrigel (BD Bioscience) in the invasion assay. RPMI media containing 10% FBS or 200 ng/mL CXCL12 in the lower compartment stimulated the cells to migrate or invade. After 24-hr incubation, the cells present on the lower surface of the membrane were counted in five random fields at 100 \times magnification. The degree of migration and invasion was adjusted based on the cell proliferation effects of FBS or CXCL12. Alternatively, cells were pretreated with an indicated inhibitor for 30 min and then loaded into the upper chambers. The inhibitors were present in both chambers for the duration of the assays.

Tumor sphere formation assay

PC cells (1×10^3 cells/mL) were plated on ultralow-attachment plates (Corning) in DMEM/F12 medium containing 1% Insulin-Transferrin-Selenium-X (Invitrogen), 2% B27 (GIBCO), 20 ng/mL epidermal growth factor and 20 ng/mL basic fibroblast growth factor (R&D systems). After up to 7 days, tumor spheres >100 μ m in diameter were counted. In the limiting-dilution assay, PC cells were plated at various seeding densities and incubated for 1 week. Each well was observed to quantify sphere formation. Clonogenic cell frequency was calculated using the Extreme Limiting Dilution Analysis software.

Statistical analysis

Significance of differences was assessed using unpaired Student's *t* test or 1-way ANOVA test followed by the Student-Newman-Keuls test. Overall survival (OS) rates were estimated using the Kaplan-Meier method and compared using

the log-rank test. Tumor metastasis rates were compared using Fisher's exact test, two tailed. Difference was considered significant if $p < 0.05$.

Results

Tpl2 enhances *in vivo* tumorigenesis and metastasis of ADI PC cells

To evaluate the clinical implication of Tpl2 in the progression and metastasis of CRPCs, we confirmed that Tpl2 mRNA levels of metastatic CRPCs ($n = 25$) were significantly higher than those of localized PCs ($n = 66$; $p < 0.001$, Supporting Information Fig. 1a) in a public database.¹⁰ Consistently, Tpl2 mRNA expression in human ADI PC cells PC3, DU145 and C4-2B cells, which exhibit *in vivo* tumorigenic/metastatic potential, was higher than that in the weakly tumorigenic/nonmetastatic 22Rv1 human ADI PC cells (Supporting Information Fig. 1b).¹⁶ The cell lines expressing the highest and lowest levels of Tpl2, PC3 and 22Rv1, respectively, were chosen for further studies. The differential expression of Tpl2 was confirmed at the protein level (Supporting Information Fig. 1c). We established Tpl2-knockdown (KD) PC3 (PC3-shTpl2) and Tpl2-overexpressing 22Rv1 (22Rv1-Tpl2 OE) stable sublines, together with corresponding controls (a scrambled shRNA for PC3-shCon and an empty vector for 22Rv1-Con). Down- and upregulation of Tpl2 was verified *in vitro* and *in vivo* (Fig. 1a).

2×10^6 PC3-shCon ($n = 13$) or PC3-shTpl2 ($n = 11$) cells were implanted in the prostate of immune-deficient male mice. When mice were euthanized upon loss of >20% body-weight or signs of serious distress, significantly longer OS was observed in the Tpl2-KD group [median (range); 58 (32–71) days] compared with the control group [19 (15–22) days](Fig. 1b, left). Sacrificed mice usually showed bilateral renal ischemic changes, hydronephrosis, bladder distension and urinary ascites. Those urinary flow blockage symptoms and larger implanted cell number than previous PC3 orthotopic animal models^{17,18} would provoke the relatively shorter OS in this study than the previous animal models. Tpl2 silencing also significantly reduced the number of spontaneous metastatic foci in periaortic lymph nodes (LNs) and lung (Fig. 1b, right). Moreover, when mice were simultaneously sacrificed at 3 weeks after tumor-cell transplantation, the Tpl2 downregulation had significantly inhibited both primary tumor formation and spontaneous metastasis (Fig. 1c). The mice injected with PC3-shTpl2 cells showed a clear margin of primary tumors in contrast to the invasive growth patterns observed in the PC3-shCon group (Fig. 1c, lower left).

To further examine whether primary tumorigenesis and spontaneous metastasis are enhanced by Tpl2 overexpression, we orthotopically implanted 2×10^6 22Rv1-Con ($n = 7$) or 22Rv1-Tpl2 OE ($n = 8$) cells in the prostate of immune-deficient male mice. As expected, 22Rv1-Tpl2 OE cells formed significantly larger prostate tumors than 22Rv1-Con cells ($p < 0.001$, Fig. 1d, upper left). Furthermore, primary

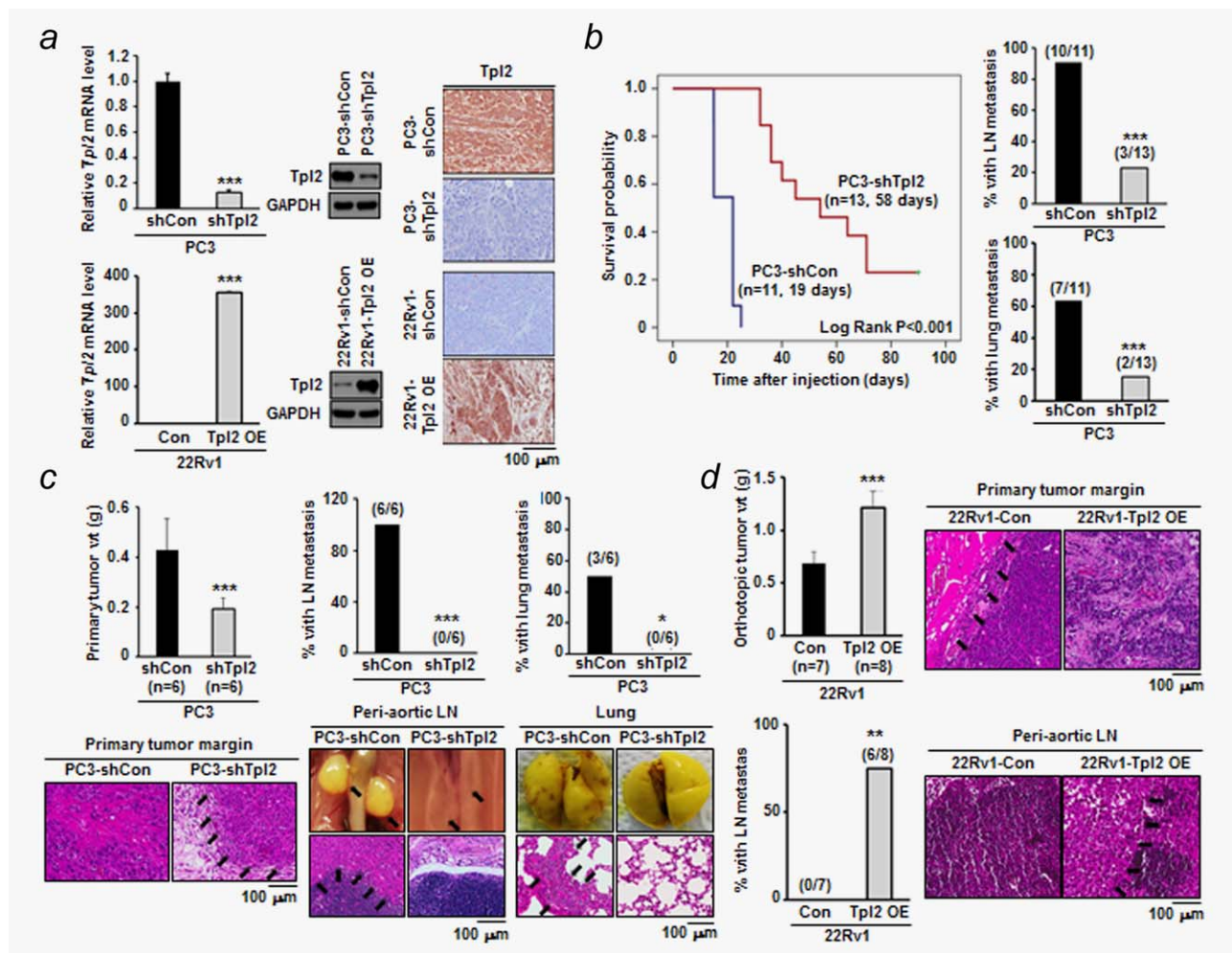


Figure 1. Tpl2 increases tumorigenic and metastatic potential of ADI PC cells *in vivo*. (a) Tpl2 knockdown and overexpression was verified using qRT-PCR ($n = 4$ for each group; left), Western blotting (middle) and immunohistochemistry against orthotopic xenograft tumors (right). One of triplicated experiments was illustrated. Internal control for qRT-PCR = 18S RNA. GAPDH=loading control. (b) Kaplan–Meier curve shows the survival rate of mice (left, mortality: >20% total body weight loss). Spontaneous periaortic LNs and lung metastasis were evaluated by histologic examination (right). (c) Primary tumor growth and spontaneous metastasis were simultaneously analyzed at 3 weeks postinjection. Data = mean \pm SEM (left). Arrows = tumor margin (left), periaortic LNs (middle upper) and metastatic foci (middle lower and right). (d) Tumor weights of orthotopic tumors and incidences of LN metastasis at 28 days postimplantation were presented. Arrows = tumor margin (upper) and metastasized tumor cells in LN (lower). * $p < 0.05$, ** $p < 0.01$ and *** $p < 0.001$.

tumors derived from 22Rv1-Tpl2 OE cells showed infiltration of cancer cells to the stroma, whereas 22Rv1-Con cells generated primary tumors with well-defined margins (Fig. 1d, upper right). At 4 weeks postimplantation no LN metastasis was detected in any mice bearing tumors derived from 22Rv1-Con cells. In contrast, 22Rv1-Tpl2 OE cells induced spontaneous metastasis to periaortic LNs in six of the eight mice ($p = 0.003$, Fig. 1d, lower). Metastatic nodules were not observed in the other organs including the lung.

The specific effects of Tpl2 on the metastatic properties of ADI PC cells were also analyzed by intracardiac injection of 2×10^5 PC3-shCon or PC3-shTpl2 cells. Survival of mice was significantly increased following Tpl2 KD [PC3-shTpl2, 84 (57–90) days; PC3-shCon, 34 (25–36) days; Supporting Information Fig. 2a]. When systemic metastasis was concur-

rently analyzed at 4 weeks after injection, the ratio of mice exhibiting distant metastases was significantly reduced in the Tpl2 KD group (Supporting Information Fig. 2a). To recapitulate bone metastasis, 2×10^5 PC3-shCon or PC3-shTpl2 cells were directly injected into the bone-marrow space of tibia. When mice were sacrificed at 3 weeks after injection, PC3-shCon cells have reproducibly generated intratibial tumors with osteolytic activity in 86% of the mice, whereas PC3-shTpl2 cells generated an intratibial mass in only 11% of injected mouse (Supporting Information Fig. 2b, $p = 0.0008$).

In vitro oncogenic effects of Tpl2 in ADI PC cells

To elucidate the underlying mechanisms, we evaluated various *in vitro* phenotypic changes in ADI PC cells in relation to Tpl2 expression. Whereas *in vitro* proliferation was

significantly impaired following Tpl2 silencing in PC3 cells, Tpl2 overexpression significantly increased the proliferation of 22Rv1 cells (Supporting Information Fig. 3a). Moreover, *in vitro* clonogenicity of PC3 cells decreased significantly when Tpl2 was silenced, whereas upregulating Tpl2 in 22Rv1 cells increased *in vitro* clonogenicity significantly (Fig. 2a). To confirm that the *in vitro* effects of shRNA-mediated Tpl2 KD depend on the kinase activity of Tpl2, the effects of a Tpl2-specific KI¹⁹ were additionally tested. Agreeing with the Tpl2-targeting shRNA results, Tpl2-specific KI potently suppressed *in vitro* proliferation (Supporting Information Fig. 3b) and clonogenicity (Supporting Information Fig. 3c) of PC3 cells. Moreover, in 22Rv1-Tpl2 OE cells, the *in vitro* effects of Tpl2 overexpression were completely reversed by the Tpl2-KI (Fig. 2b).

We further tested the effects of Tpl2 expression on ADI PC cells by using *in vitro* migration and invasion assays. As shown in Fig. 2c (top), Tpl2 KD significantly attenuated the migration/invasion of PC3 cells. Conversely, 22Rv1-Tpl2 OE cells showed significantly higher migration/invasion capacities than 22Rv1-Con cells (Fig. 2c, bottom). The inhibitory effects of the Tpl2-targeting shRNA were reproduced by the Tpl2-KI (Fig. 2d). We analyzed whether these aggravated characteristics are related to epithelial-mesenchymal transition (EMT). Interestingly, cellular morphologies of Tpl2 KD PC3 and Tpl2 overexpressing 22Rv1 sublines, transformed into epithelial and mesenchymal cell-like, respectively (Fig. 3a). These morphological changes were accompanied with increased E-cadherin and diminished vimentin expression in the case of Tpl2 KD, with the reverse effects being observed with Tpl2 overexpression (Fig. 3b). Moreover, the expression of ZEB1, a master transcription factor of EMT,²⁰ was positively correlated with the expression of Tpl2 (Fig. 3b). The correlations between the expression of Tpl2 and of EMT-related molecules were verified in both *in vivo* orthotopic xenografts (Fig. 3c) and MSKCC clinical dataset ($n = 127$, Fig. 3d).

In vitro Tpl2 KD effects on PC3 cells were reproduced using C4-2B cells. C4-2B cells express androgen receptor but proliferate without androgen, therefore, simulate androgen receptor expressing ADI PCs more precisely than PC3 cells.²¹ Androgen withdrawal in the culture medium induced upregulation of Tpl2 in C4-2B cells (Supporting Information Figs. 4a and 4b). In the androgen depletion status, Tpl2 KD significantly reduced the *in vitro* clonogenicity (Supporting Information Fig. 4d) and migration/invasion (Supporting Information Fig. 4e) of C4-2B cells. In contrast, *in vitro* proliferation of C4-2B cells was not significantly impaired by Tpl2 silencing (Supporting Information Fig. 4c). Since effects of Tpl2-KD was reproduced in two independent ADI PC cell lines, the effects of Tpl2 silencing would not be cell line-specific.

Tpl2 regulates stem-like characteristics of ADI PC cells

Recently, induction of EMT has been shown to generate cells with stem-like properties,²² and CSCs have been shown to exhibit EMT-like molecular phenotypes.²³ Since we observed

that Tpl2 strongly promotes *in vitro* clonogenicity, a vital property of stemness, we hypothesized that multiple *in vitro* and *in vivo* effects of Tpl2 on ADI PC cells could be mediated by enhanced cancer stemness.

Since *in vitro* sphere formation is widely considered to reflect the stemness, ADI PC cells were plated in a serum-free suspension culture system to make tumor spheres. PC3-shCon cells formed spheres (>100 μm diameter), but treatment with both Tpl2-specific shRNA (Fig. 4a) and KI (Fig. 4b) significantly reduced the numbers of spheres. By contrast, in 22Rv1 cells, the number of spheres increased significantly following Tpl2 overexpression (Fig. 4a), and this enhanced ability was completely reversed by Tpl2-KI (Fig. 4b). Furthermore, when we performed *in vitro* limiting-dilution assays to determine the ratio of clonogenic cancer cells, expression of the Tpl2-targeting shRNA in PC3 cells significantly decreased the ratio; conversely, Tpl2 overexpression in 22Rv1 cells significantly increased the ratio (Fig. 4c).

In addition, to examine whether Tpl2 is associated with the chemoresistance, which is another key property of CSCs,^{24,25} we compared the sensitivity of PC3-shCon and PC3-shTpl2 cells to docetaxel *in vitro*. After 72-hr docetaxel treatment, the viability of PC3-shCon cells was significantly higher than that of PC3-shTpl2 cells (Supporting Information Fig. 5). We also screened for changes in stemness-related phenotypic markers in relation to changes in Tpl2 expression. Upregulation of Tpl2 in 22Rv1 cells substantially increased the expression of CD44 and Bmi-1 *in vitro* (Fig. 4d) and *in vivo* (Fig. 4e), whereas Tpl2 depletion in PC3 cells produced the opposite effects (Figs. 4d and 4e). It has been reported that CD44^{high} subpopulations contained CSC populations in PC,^{5,26} demonstrating that CD44^{high} PC cells are more proliferative, clonogenic, tumorigenic and metastatic than the isogenic CD44^{low} cells.⁵ The expressional changes in CD44 were also confirmed by flow cytometric analysis (Supporting Information Fig. 6), which showed that CD44 expressional changes occurred in the whole population. Moreover, the ALDH activity-positive (ALDH⁺) population was decreased in PC3-shTpl2 cells, whereas Tpl2 upregulation in 22Rv1 cells increased the ratio (Supporting Information Fig. 7).

The most convincing demonstration of stemness is enhanced tumor-initiating capacity *in vivo*. We conducted orthotopic tumor development experiments by using various numbers of viable ADI-PC cells. In agreement with the *in vitro* data, Tpl2 depletion in PC3 cells exhibited 502-fold lower *in vivo* tumor initiating cell (TIC) frequency compared with that of the control group, whereas in 22Rv1 cells, Tpl2 overexpression led to a 243-fold increase in the TIC frequency (Fig. 4f). Moreover, not only primary tumor formation but also spontaneous LN metastasis was dramatically influenced by Tpl2 (Fig. 4f).

FAK and Akt mediate oncogenic effects of Tpl2 in ADI PC cells

The aforementioned results indicate that Tpl2 is a critical factor that promotes the acquisition of tumorigenic and

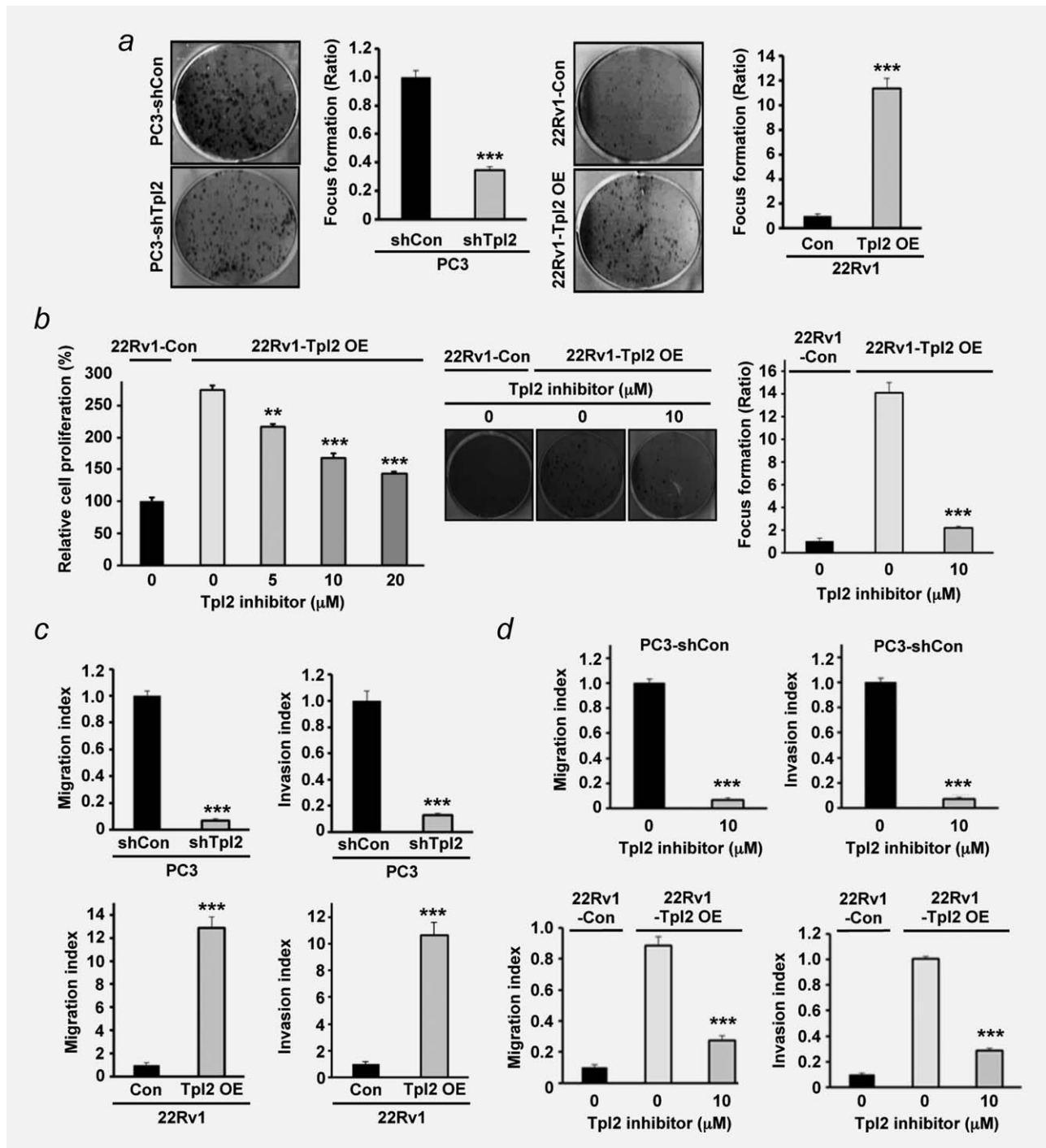


Figure 2. In vitro oncogenic effects of Tpl2 on ADI PC cells. (a) Clonal growth of ADI PC cells was compared using focus formation assay. (b) Effects of Tpl2-KI treatment on proliferation (left) and clonogenicity (right) of 22Rv1-Tpl2 OE cells. (c and d) Effect of Tpl2 expression (c) and KI (d) on *in vitro* cell migration and invasion. Data = mean \pm SD, $n = 4$ for each group (a and d). One of triplicated experiments was illustrated for (a) and (d). ** $p < 0.01$ and *** $p < 0.001$.

metastatic potential in ADI PC cells. To address the mechanism, we investigated the activation status of several oncogenic signaling pathways that regulate EMT and stem cell-like traits. Among these pathways, the activation of FAK and Akt has been reported to be closely associated with cell pro-

liferation, anoikis resistance, migration, invasion and stemness of PC cells.^{27–31} In PC3-shTpl2 cells, depletion of Tpl2 led to a remarkable decrease in the phosphorylation levels of FAK and Akt, compared with those of control cells (Fig. 5a). By contrast, Tpl2 reconstitution in 22Rv1 cells dramatically

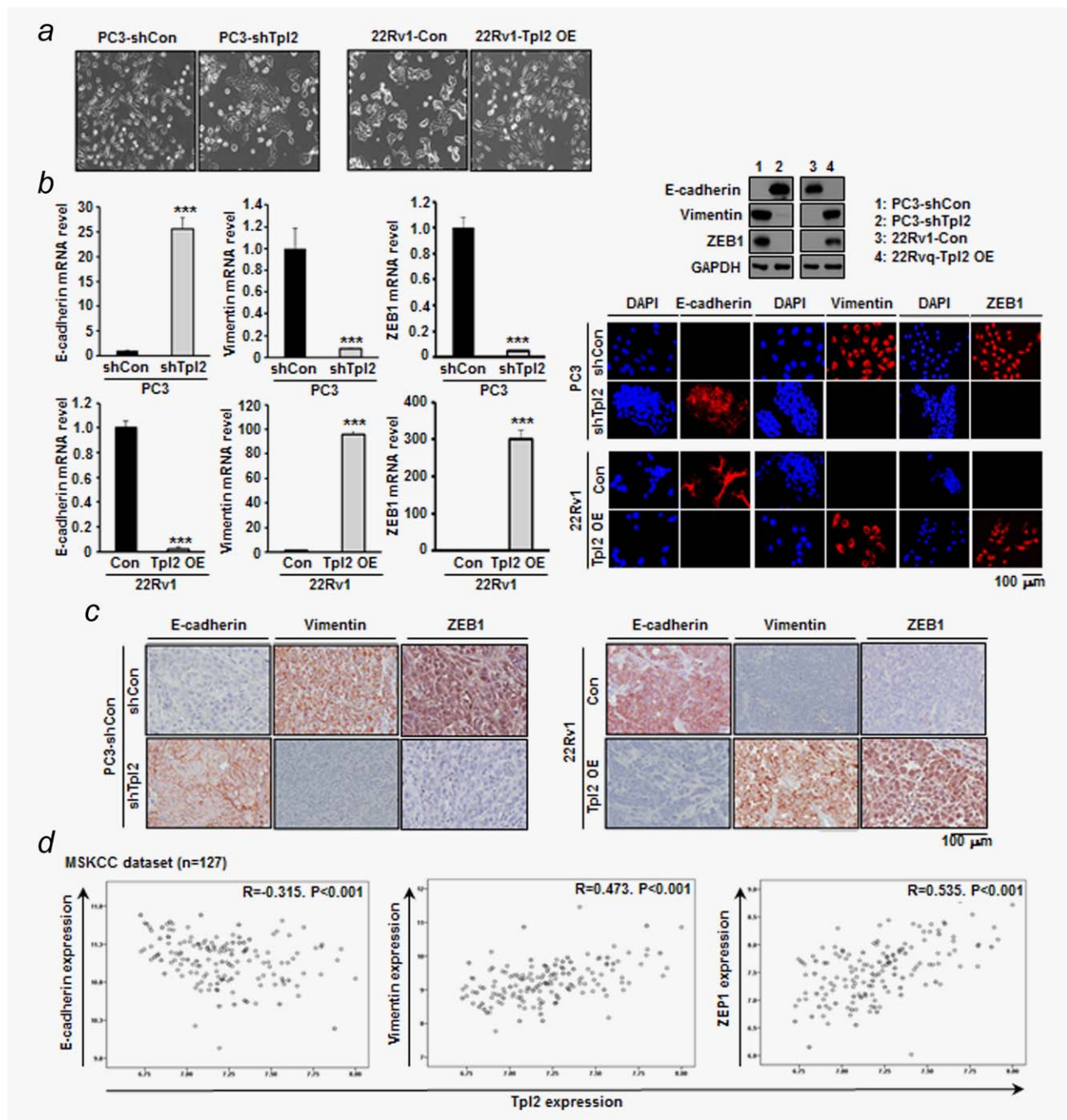


Figure 3. EMT of ADI PC cells was induced by Tpl2. (a) Morphological transformation of ADI PC cells upon Tpl2 manipulation. (b) The mRNA and protein levels of EMT makers were determined by qRT-PCR (right, $n = 4$ for each group, data = mean \pm SD), Western blotting (left upper) and immunocytochemistry (left lower). DAPI = nuclei. (c) E-cadherin, vimentin and ZEB1 expression were determined by immunohistochemistry in orthotopic xenograft tumors. One of triplicated experiments was illustrated for (a) and (c). (d) Correlation analysis between E-cadherin/vimentin/ZEB1 and Tpl2 expression in the MSKCC dataset. $R =$ Spearman's correlation coefficient. $***p < 0.001$. [Color figure can be viewed in the online issue, which is available at wileyonlinelibrary.com.]

enhanced the activation of FAK and Akt (Fig. 5a). However, the expected activation of ERK and JNK, major downstream signaling components of Tpl2, was not observed in our Tpl2-manipulated ADI PC cells (Fig. 5a). Interestingly, the expression of FAK (Fig. 5a and Supporting Information Fig. 8) was also positively associated with Tpl2 expression, which, how-

ever, did not markedly change Akt expression (Fig. 5a). The activation of FAK and Akt and the upregulation of FAK were confirmed in orthotopic xenografts (Fig. 5b).

To determine whether the activation of FAK and Akt is required for Tpl2-mediated effects on ADI PC cells, effects of specific FAK and Akt inhibitors on *in vitro* phenotypes

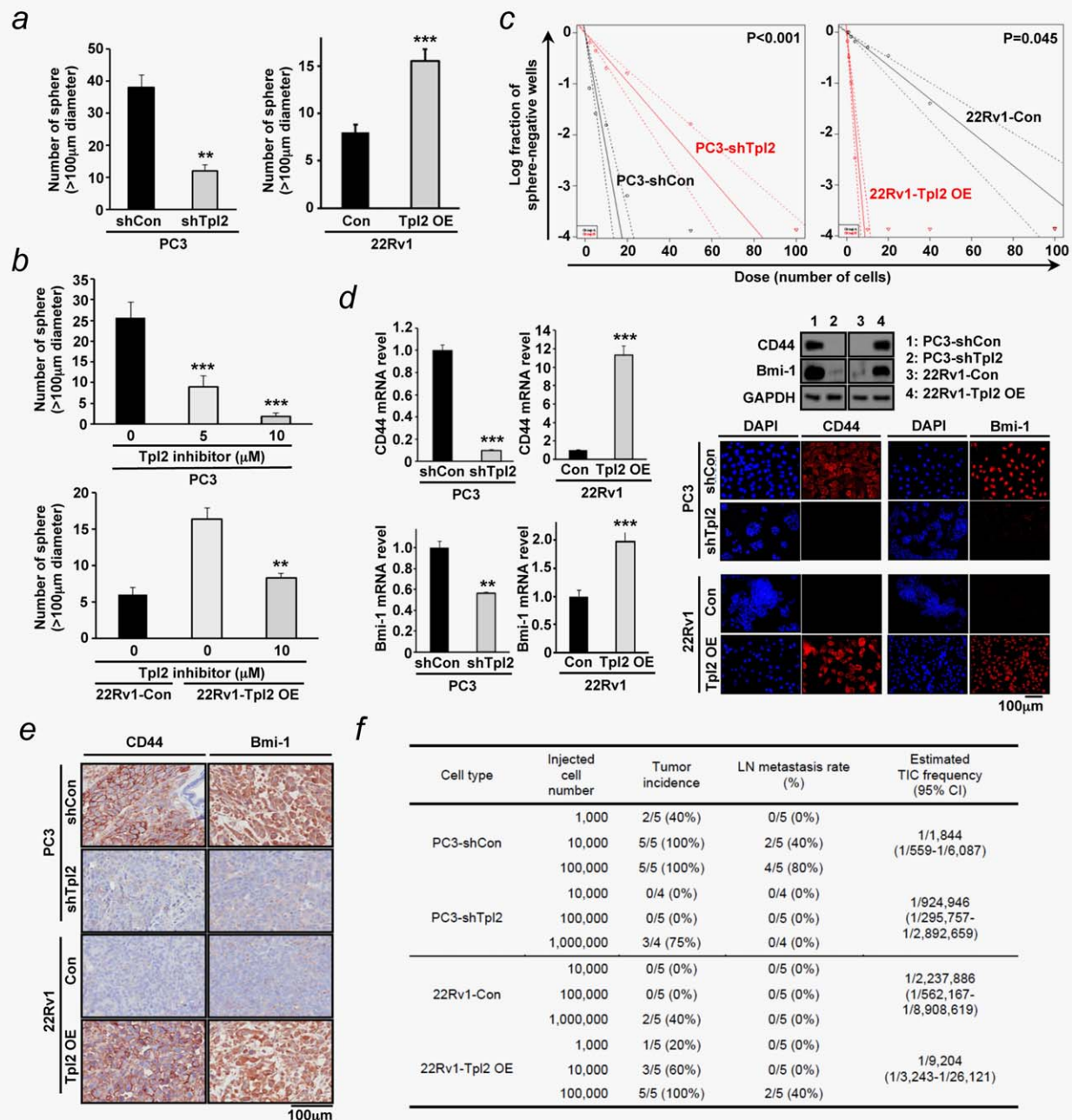


Figure 4. Involvement of Tpl2 in the stem-cell like characteristics of ADI PC cells. (a) Sphere-formation of ADI PC cells was analyzed. (b) The effects of Tpl2-KI on tumor sphere-forming ability of ADI PC cells *in vitro*. Data = mean \pm SD, $n = 4$ for each group (a and b). (c) *In vitro* limiting dilution assays were performed to determine clonogenic potentials of ADI PC cells ($n = 3$ for each group). (d) The mRNA and protein expression of CD44 and Bmi-1 of ADI PC cells were analyzed by qRT-PCR ($n = 4$ for each group, data = mean \pm SD, left), Western blot (right upper) and immunocytochemistry (right lower), *in vitro*. DAPI=nuclei. One of triplicated experiments was illustrated for (a) and (d). ** $p < 0.01$ and *** $p < 0.001$. (e) Expression of CD44 and Bmi-1 were analyzed by immunohistochemistry in orthotopic xenograft tumors. (f) *In vivo* tumorigenicity titration assay was performed by orthotopic injection of various numbers of ADI PC cells. [Color figure can be viewed in the online issue, which is available at wileyonlinelibrary.com.]

of ADI PC cells were assessed. Both PF-573,228 (an ATP-competitive, reversible inhibitor of FAK)³² and GSK690,693 (an ATP-competitive, pan-Akt inhibitor)³³ significantly suppressed proliferation (Supporting Information Fig. 9), clonogenicity (Fig. 5c) and migration/invasion (Fig.

5d) of PC3 cells. Demonstrating specificity further, the proliferation (Supporting Information Fig. 9), clonogenicity (Fig. 5c) and migration/invasion (Fig. 5d) of 22Rv1 cells that were increased by Tpl2 overexpression were potently reversed by the specific inhibitors.

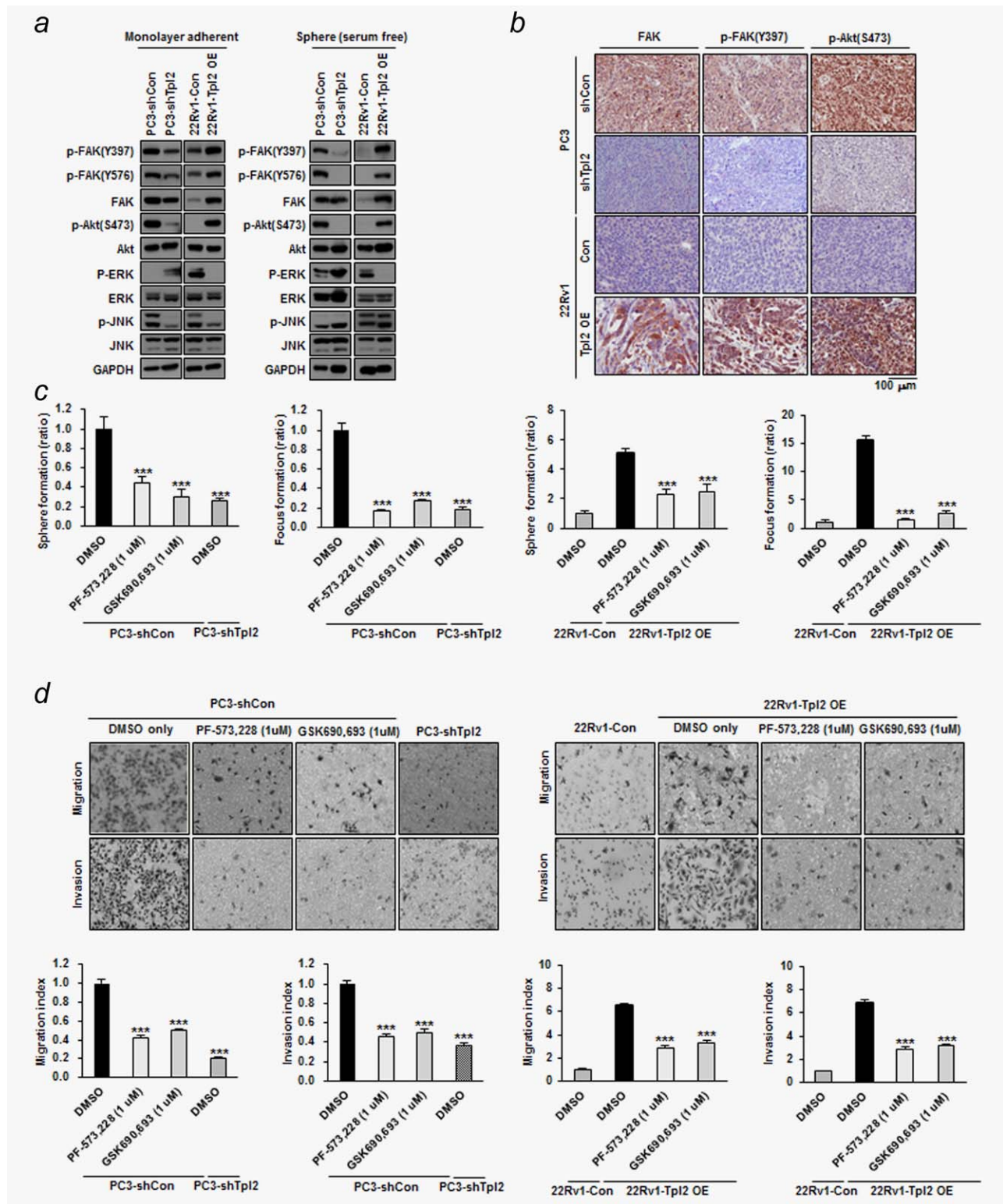


Figure 5. The activation of FAK and Akt signaling mediates oncogenic effects of Tpl2 in ADI PC cells. (a) Comparison of oncogenic signaling pathways in relation to Tpl2 expression. GAPDH = loading control. (b) Levels of FAK, p-FAK(Y397) and p-Akt(S473) were detected by immunohistochemistry in orthotopic xenograft tumors. (c) The effects of FAK (PF-573,228, 1 μ M) and Akt (GSK690,693, 1 μ M) specific inhibitor on the clonogenicity of ADI PC cells. (d) Inhibition of FAK (PF-573,228, 1 μ M) and Akt (GSK690,693, 1 μ M) activity suppressed *in vitro* migration and invasion of ADI PC cells. Data = mean \pm SD, $n = 4$ for each group (c and d). One of triplicated experiments was illustrated for (a) and (d). *** $p < 0.001$. [Color figure can be viewed in the online issue, which is available at wileyonlinelibrary.com.]

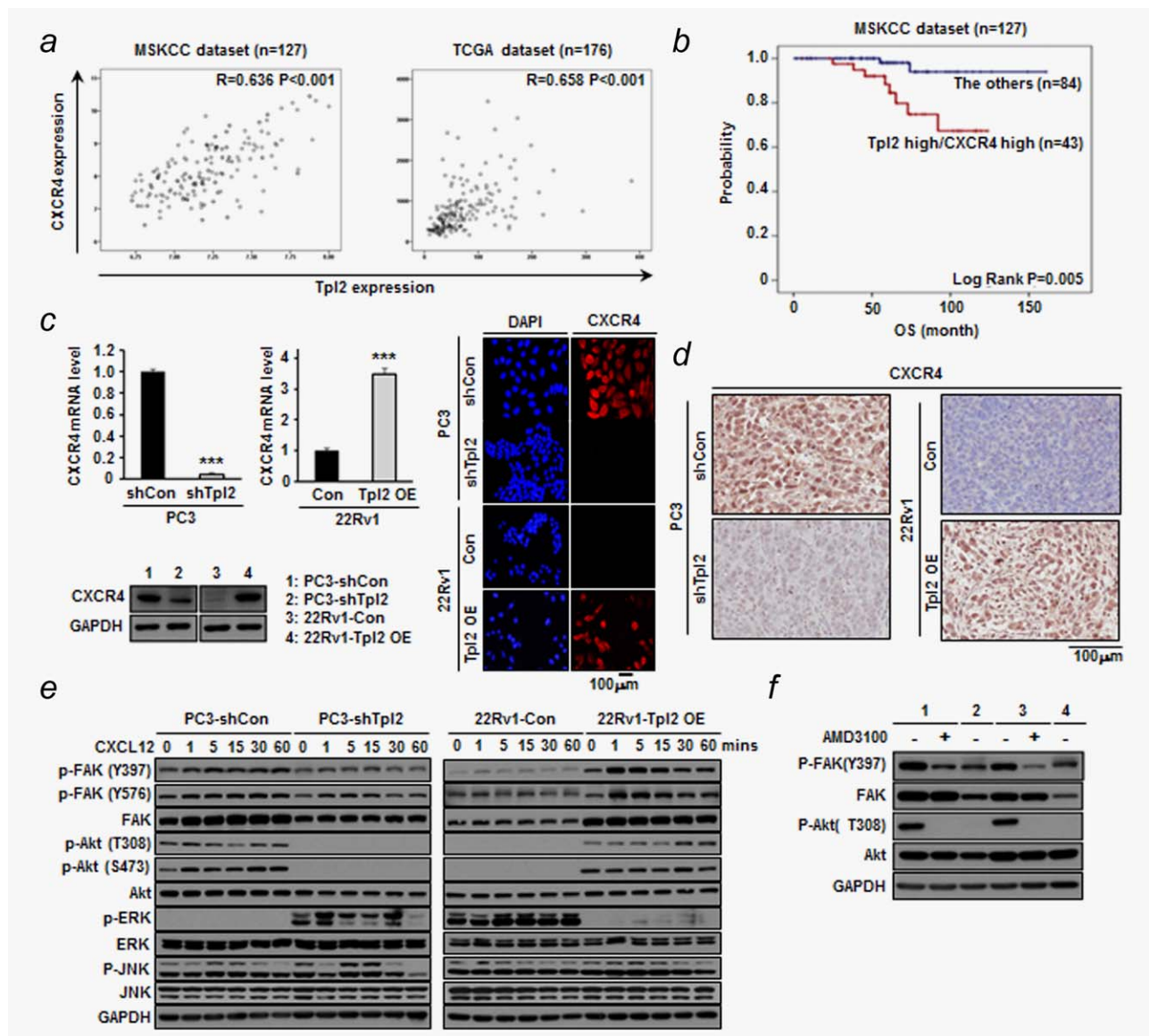


Figure 6. Tpl2 upregulated CXCR4 expression of ADI PC cells and potentiated CXCR4 signaling pathway. (a) Correlation analysis between Tpl2 and CXCR4 mRNA levels in human PCs. R = Spearman's correlation coefficient. (b) Kaplan–Meier graphs represent the probability of cumulative OS of human PCs (MSKCC dataset). (c) Expression of CXCR4 mRNA and protein in relation to Tpl2 levels in PC3 and 22Rv1 cells was evaluated by qRT-PCR ($n = 4$ for each group, data = mean \pm SD, left upper), Western blot (left lower) and immunocytochemistry (right). DAPI = nuclei. (d) CXCR4 expression was analyzed by immunohistochemistry in orthotopic xenograft tumors. (e) Changes in CXCL12/CXCR4-mediated signal transduction following Tpl2 silencing in PC3 cells (left) and Tpl2 reconstitution in 22Rv1 cells (right) upon *in vitro* stimulation by CXCL12 (200 ng/mL) were analyzed by Western blotting. GAPDH = loading control. (f) Effects of CXCR4 inhibition (AMD3100, 10 μ M) on the FAK expression of ADI PC cells were analyzed by Western blotting. GAPDH = loading control. One of triplicated experiments was illustrated for C-F. *** $p < 0.001$. [Color figure can be viewed in the online issue, which is available at wileyonlinelibrary.com.]

Tpl2 activates FAK and Akt through the CXCL12/CXCR4 signaling pathway in ADI PC cells

FAK and Akt were found to function downstream from Tpl2, but how Tpl2 signals to these effectors is unknown. Previously, we reported that Tpl2 enhances the tumorigenic and metastatic potential of ccRCC through the CXCL12/CXCR4 signaling pathway.¹³ CXCR4 is activated by its exclusive ligand CXCL12, which leads to the activation of diverse intracellular

signaling pathways including the Akt pathway.³⁴ Moreover, CXCL12 evoked FAK upregulation and enhanced FAK phosphorylation.³⁵ Therefore, CXCR4 could be a missing link between Tpl2 and FAK/Akt.

We examined the association of CXCR4 and Tpl2 expression in two independent PC databases, which revealed that their expression is significantly correlated in human PCs (Fig. 6a). Moreover, for Tpl2 and CXCR4 as a two-gene classifier,

we defined the PCs that exhibited CXCR4 and Tpl2 expression above the averages across all PCs in the MSKCC dataset as Tpl2 high/CXCR4 high. Although Tpl2 or CXCR4 expression level alone could not differentiate the clinical outcome of PC patients ($p = 0.16$ and $p = 0.070$, respectively, Supporting Information Fig. 10), Tpl2 high/CXCR4 high PCs showed significantly worse OS than the other PCs (Fig. 6b), suggesting that enhanced Tpl2 activity could be associated with worse clinical prognosis as a result of CXCR4 upregulation.

Supporting the clinical observations, Tpl2 silencing in PC3 cells resulted in significantly decreased CXCR4 expression and reconstitution of Tpl2 in 22Rv1 cells upregulated CXCR4 expression *in vitro* (Fig. 6c) and *in vivo* (Fig. 6d). Functionally, treating PC3-shCon cells with CXCL12 induced FAK and Akt phosphorylation, which was dramatically inhibited by shRNA-mediated Tpl2 KD (Fig. 6e, left). By contrast, Tpl2 overexpression in 22Rv1 cells potentiated CXCL12-mediated FAK and Akt phosphorylation (Fig. 6e, right). However, FAK expression was not significantly altered by exposure to CXCL12 for 60 min, and activation of ERK and JNK was not observed following either Tpl2 overexpression or CXCL12 treatment (Fig. 6e).

To confirm that CXCR4 activation is an essential part of the diverse effects produced by Tpl2 on ADI PC cells, we utilized AMD3100, a specific CXCR4 antagonist. At a molecular level, the CXCR4 antagonist potentially impaired the phosphorylation of FAK and Akt induced by CXCL12 in PC3-shCon and 22Rv1-Tpl2 OE cells, but FAK expression itself was not changed (Fig. 6f). Although the CXCR4 antagonist had no effect on the growth of ADI PC cells *in vitro* (data not shown), clonogenicity of PC3 cells were strongly suppressed by the CXCR4 antagonist (Supporting Information Figs. 11a and 11b). More importantly, the increased clonogenicity of 22Rv1 cells induced by Tpl2 overexpression was eliminated by CXCR4 inhibition (Supporting Information Figs. 11c and 11d). Furthermore, although PC3-shCon and 22Rv1-Tpl2 OE cells showed prominent chemotaxis and chemoinvasion toward CXCL12, CXCL12 failed to induce these behaviors in PC3 Tpl2 KD cells (Supporting Information Figs. 11e and 11f). Moreover, the enhancement of CXCL12-dependent chemotaxis and chemoinvasion in Tpl2-overexpressing 22Rv1 cells was completely reversed by the CXCR4 specific antagonist (Supporting Information Fig. 11f).

Discussion

Tpl2 has been implicated in the progression of PC to the CRPC stage,¹⁵ but the molecular pathophysiology of Tpl2-stimulated tumor progression and metastasis of CRPC remains poorly elucidated. This study has demonstrated the functional roles of Tpl2 in tumor progression and metastasis of CRPC, promoting EMT and maintaining stemness, which would enhance cell proliferation, clonogenicity, migration and invasion. Our mechanistic studies revealed that Tpl2 regulates the tumorigenic and metastatic potential of ADI PC cells at least in part by upregulating CXCR4

and FAK and consequently activating FAK/Akt downstream signaling pathways (Supporting Information Fig. 12). The experimental results were strongly supported by the results of our analysis of two independent clinical PC databases (MSKCC and TCGA), which enhance the clinical relevance of this study.

The phenotypic association between EMT and tumor-initiating properties has been firmly established.²² However, the underlying common mechanisms that regulate these two independent characteristics remain largely unknown. Recently, activation of the PI3K/Akt signaling pathway is associated with enhanced PC cell proliferation, invasion, metastasis, chemo-/radio-resistance, stemness and EMT, which would indicate that PI3K-targeting modalities could be a promising method to eliminate CSCs and to overcome treatment-resistance of PC.^{36–38} In this study, we identified Tpl2 as a master regulator that controls the EMT and stemness of CRPC. Although Tpl2 protein kinase does not directly phosphorylate PI3K, PI3K is a downstream component of FAK/Akt and CXCL12/CXCR4 signaling pathways.

Tpl2 protein kinase can directly activate the MAP and JNK kinases.^{10,14,15,39} However, the expected changes in ERK and JNK phosphorylation were not induced by either downregulation or overexpression of Tpl2 in ADI PC cells in this study although the mechanisms underlying the differential Tpl2-mediated downstream signaling was not elucidated in detail. Instead, upregulation of FAK and CXCR4 and activation of FAK/Akt and CXCL12/CXCR4 signaling pathways were associated with Tpl2 expression in ADI PC cells. The activation of FAK and Akt has been reported to be closely associated with cell proliferation, anoikis resistance, migration, invasion and stemness of PC cells.^{27–31,40–42} CXCR4 leads to the activation of diverse intracellular signaling pathways including the Akt pathway,^{34,43,44} and CXCL12 evoked increased expression of FAK and enhanced FAK phosphorylation.³⁵ Furthermore, it has been established that the tumorigenic and metastatic process of PC is regulated by CXCL12/CXCR4 axis. CXCR4 expression increases during the progression of PC and is associated with poor survival of PC patients.^{45,46} In a previous study,¹³ we demonstrated that Tpl2 promotes the progression and metastasis of ccRCC through CXCL12/CXCR4 signaling pathways. In contrast to its function in urogenital tumors, Tpl2 acts as a tumor suppressor gene in lung carcinogenesis through p53 response to genotoxic stress.⁴⁷ Therefore, Tpl2 exerts its unique functions according to the characteristic molecular environments of biological systems. Specifically, in urogenital cancers, Tpl2 acts as a principal driver of the progression and metastasis by activating FAK/Akt and CXCL12/CXCR4 signaling pathways.

Developing therapeutic strategies for chemoresistant CRPC remains a challenging problem in clinical oncology because no optimal therapeutic target has been identified. Recently, docetaxel treatment was shown to constitutively activate the CXCR4, ERK1/2 and c-Myc signaling loop in docetaxel-resistant residual PC cells.⁴⁸ The CXCL12/CXCR4

pathway, in particular, is highly activated in the CD133⁺/CD44⁺ prostate progenitor population, which is self-renewing and exhibits strong *in vivo* tumorigenic potential.^{5,6,36} Combining a PC CSC-targeting CXCR4 antagonist, AMD3100, with a conventional chemotherapeutic drug was considerably more effective than monotherapy in eradicating tumors.⁴⁹ Our data suggest that Tpl2 is a potential therapeutic target for metastatic and docetaxel-resistant ADI PC and that Tpl2 activates CXCL12/CXCR4 signaling. Moreover, Tpl2 directly upregulated the expression of FAK and CXCR4. Although the CXCR4-specific inhibitor suppressed the clonogenicity, migration and invasion of ADI PC cells, it did not affect cell proliferation in this study. Therefore, using strategies to target Tpl2, an upstream regulator of CXCL12/CXCR4 signaling, could be more effective.

References

- Siegel R, Naishadham D, Jemal A. Cancer statistics, 2012. *CA Cancer J Clin* 2012;62:10–29.
- Birtle A. Maximizing survival in metastatic castrate-resistant prostate cancer: a clinical viewpoint. *Expert Rev Anticancer Ther* 2013;13:89–99.
- Semenas J, Allegrucci C, Boorjian SA, et al. Overcoming drug resistance and treating advanced prostate cancer. *Curr Drug Targets* 2012;13:1308–23.
- Reya T, Morrison SJ, Clarke MF, et al. Stem cells, cancer, and cancer stem cells. *Nature* 2001;414:105–11.
- Patrawala L, Calhoun T, Schneider-Broussard R, et al. Highly purified CD44⁺ prostate cancer cells from xenograft human tumors are enriched in tumorigenic and metastatic progenitor cells. *Oncogene* 2006;25:1696–708.
- Dubrovskaya A, Elliott J, Salamone RJ, et al. Combination therapy targeting both tumor-initiating and differentiated cell populations in prostate carcinoma. *Clin Cancer Res* 2010;16:5692–702.
- Blum R, Gupta R, Burger PE, et al. Molecular signatures of prostate stem cells reveal novel signaling pathways and provide insights into prostate cancer. *PLoS One* 2009;4:e5722.
- Hurt EM, Kawasaki BT, Klarmann GJ, et al. CD44⁺ CD24⁽⁻⁾ prostate cells are early cancer progenitor/stem cells that provide a model for patients with poor prognosis. *Br J Cancer* 2008;98:756–65.
- Lukacs RU, Memarzadeh S, Wu H, et al. Bmi-1 is a crucial regulator of prostate stem cell self-renewal and malignant transformation. *Cell Stem Cell* 2010;7:682–93.
- Yu YP, Landsittel D, Jing L, et al. Gene expression alterations in prostate cancer predicting tumor aggression and preceding development of malignancy. *J Clin Oncol* 2004;22:2790–9.
- Hatziaepostolou M, Polytaichou C, Panutsopoulos D, et al. Proteinase-activated receptor-1-triggered activation of tumor progression locus-2 promotes actin cytoskeleton reorganization and cell migration. *Cancer Res* 2008;68:1851–61.
- Yang Y, Wang X, Hawkins CA, et al. Structural basis of focal adhesion localization of LIM-only adaptor PINCH by integrin-linked kinase. *J Biol Chem* 2009;284:5836–44.
- Lee HW, Joo KM, Lim JE, et al. Tumor progression locus 2 (Tpl2) kinase contributes tumor growth and metastasis of clear cell renal cell carcinoma. *Mol Cancer Res* 2013;11:1375–86.
- Lee KM, Lee KW, Bode AM, et al. Tpl2 is a key mediator of arsenite-induced signal transduction. *Cancer Res* 2009;69:8043–9.
- Jeong JH, Bhatia A, Toth Z, et al. TPL2/COT/ MAP3K8 (TPL2) activation promotes androgen depletion-independent (ADI) prostate cancer growth. *PLoS One* 2011;6:e16205.
- Thalmann GN, Sikes RA, Wu TT, et al. LNCaP progression model of human prostate cancer: androgen-independence and osseous metastasis. *Prostate* 2000;44:91–103.
- Tuomela JM, Valtala MP, Vaananen K, et al. Alendronate decreases orthotopic PC-3 prostate tumor growth and metastasis to prostate-draining lymph nodes in nude mice. *BMC Cancer* 2008;8:81.
- Davies MA, Kim SJ, Parikh NU, et al. Adenoviral-mediated expression of MMAC/PTEN inhibits proliferation and metastasis of human prostate cancer cells. *Clin Cancer Res* 2002;8:1904–14.
- Tanaka S, Nakamura K, Takahashi N, et al. Role of RANKL in physiological and pathological bone resorption and therapeutics targeting the RANKL-RANK signaling system. *Immunol Rev* 2005;208:30–49.
- Thiery JP, Aclouque H, Huang RY, et al. Epithelial–mesenchymal transitions in development and disease. *Cell* 2009;139:871–90.
- Thalmann GN, Anezinis PE, Chang SM, et al. Androgen-independent cancer progression and bone metastasis in the LNCaP model of human prostate cancer. *Cancer Res* 1994;54:2577–81.
- Mani SA, Guo W, Liao MJ, et al. The epithelial–mesenchymal transition generates cells with properties of stem cells. *Cell* 2008;133:704–15.
- Kelly K, Yin JJ. Prostate cancer and metastasis initiating stem cells. *Cell Res* 2008;18:528–37.
- Maitland NJ, Collins A. A tumour stem cell hypothesis for the origins of prostate cancer. *BJU Int* 2005;96:1219–23.
- Loriot Y, Massard C, Gross-Goupil M, et al. The interval from the last cycle of docetaxel-based chemotherapy to progression is associated with the efficacy of subsequent docetaxel in patients with prostate cancer. *Eur J Cancer* 2010;46:1770–2.
- Patrawala L, Calhoun-Davis T, Schneider-Broussard R, et al. Hierarchical organization of prostate cancer cells in xenograft tumors: the CD44⁺alpha2beta1⁺ cell population is enriched in tumor-initiating cells. *Cancer Res* 2007;67:6796–805.
- Cicchini C, Laudadio I, Citarella F, et al. TGFbeta-induced EMT requires focal adhesion kinase (FAK) signaling. *Exp Cell Res* 2008;314:143–52.
- Slack-Davis JK, Hershey ED, Theodorescu D, et al. Differential requirement for focal adhesion kinase signaling in cancer progression in the transgenic adenocarcinoma of mouse prostate model. *Mol Cancer Ther* 2009;8:2470–7.
- Parsons JT, Slack-Davis J, Tilghman R, et al. Focal adhesion kinase: targeting adhesion signaling pathways for therapeutic intervention. *Clin Cancer Res* 2008;14:627–32.
- Taylor BS, Schultz N, Hieronymus H, et al. Integrative genomic profiling of human prostate cancer. *Cancer Cell* 2010;18:11–22.
- Shen MM, Abate-Shen C. Pten inactivation and the emergence of androgen-independent prostate cancer. *Cancer Res* 2007;67:6535–8.
- Slack-Davis JK, Martin KH, Tilghman RW, et al. Cellular characterization of a novel focal adhesion kinase inhibitor. *J Biol Chem* 2007;282:14845–52.
- Rhodes N, Heerding DA, Duckett DR, et al. Characterization of an Akt kinase inhibitor with potent pharmacodynamic and antitumor activity. *Cancer Res* 2008;68:2366–74.
- Chinni SR, Sivalogan S, Dong Z, et al. CXCL12/CXCR4 signaling activates Akt-1 and MMP-9 expression in prostate cancer cells: the role of bone microenvironment-associated CXCL12. *Prostate* 2006;66:32–48.
- Engl T, Relja B, Marian D, et al. CXCR4 chemokine receptor mediates prostate tumor cell adhesion through alpha5 and beta3 integrins. *Neoplasia* 2006;8:290–301.
- Dubrovskaya A, Kim S, Salamone RJ, et al. The role of PTEN/Akt/PI3K signaling in the maintenance and viability of prostate cancer stem-like cell populations. *Proc Natl Acad Sci USA* 2009;106:268–73.
- Ni J, Cozzi P, Hao J, et al. Epithelial cell adhesion molecule (EPCAM) is associated with prostate cancer metastasis and chemo/radioresistance via

Acknowledgements

This research was supported by a grant of the Korea Health Technology R&D Project through the Korea Health Industry Development Institute (KHIDI) funded by the Ministry of Health & Welfare, Republic of Korea (HI09C1552) (DH Nam). This research was supported by Samsung Medical Center grant (GFO1140011) (DH Nam), Global Frontier Project grant (NRF-M3A6A4-2010-0029785) of National Research Foundation funded by the Ministry of Science, ICT & Future Planning (MSIP) of Korea (SH Kim), and the Samsung Biomedical Research Institute grant no. SMX-1131281 (KM Joo).

- the PI3K/Akt/mTOR signaling pathway. *Int J Biochem Cell Biol* 2013;45:2736–48.
38. Chang L, Graham PH, Hao J, et al. Acquisition of epithelial–mesenchymal transition and cancer stem cell phenotypes is associated with activation of the PI3K/Akt/mTOR pathway in prostate cancer radioresistance. *Cell Death Dis* 2013;4:e875.
 39. Das S, Cho J, Lambertz I, et al. Tpl2/cot signals activate ERK, JNK, and NF-kappaB in a cell-type and stimulus-specific manner. *J Biol Chem* 2005; 280:23748–57.
 40. Slack JK, Adams RB, Rovin JD, et al. Alterations in the focal adhesion kinase/Src signal transduction pathway correlate with increased migratory capacity of prostate carcinoma cells. *Oncogene* 2001;20:1152–63.
 41. Tremblay L, Hauck W, Aprikan AG, et al. Focal adhesion kinase (pp125FAK) expression, activation and association with paxillin and p50CSK in human metastatic prostate carcinoma. *Int J Cancer* 1996;68:164–71.
 42. Yan W, Fu Y, Tian D, et al. PI3 kinase/Akt signaling mediates epithelial–mesenchymal transition in hypoxic hepatocellular carcinoma cells. *Biochem Biophys Res Commun* 2009;382:631–6.
 43. Chinni SR, Yamamoto H, Dong Z, et al. CXCL12/CXCR4 transactivates HER2 in lipid rafts of prostate cancer cells and promotes growth of metastatic deposits in bone. *Mol Cancer Res* 2008;6:446–57.
 44. Kukreja P, Abdel-Mageed AB, Mondal D, et al. Up-regulation of CXCR4 expression in PC-3 cells by stromal-derived factor-1alpha (CXCL12) increases endothelial adhesion and transendothelial migration: role of MEK/ERK signaling pathway-dependent NF-kappaB activation. *Cancer Res* 2005;65:9891–8.
 45. Mochizuki H, Matsubara A, Teishima J, et al. Interaction of ligand-receptor system between stromal-cell-derived factor-1 and CXC chemokine receptor 4 in human prostate cancer: a possible predictor of metastasis. *Biochem Biophys Res Commun* 2004;320:656–63.
 46. Akashi T, Koizumi K, Tsuneyama K, et al. Chemokine receptor CXCR4 expression and prognosis in patients with metastatic prostate cancer. *Cancer Sci* 2008;99:539–42.
 47. Gkirtzimanaki K, Gkouskou KK, Oleksiewicz U, et al. TPL2 kinase is a suppressor of lung carcinogenesis. *Proc Natl Acad Sci USA* 2013;110: E1470–9.
 48. Hatano K, Yamaguchi S, Nimura K, et al. Residual prostate cancer cells after docetaxel therapy increase the tumorigenic potential via constitutive signaling of CXCR4, ERK1/2 and c-Myc. *Mol Cancer Res* 2013;11:1088–100.
 49. Dubrovskaya A, Elliott J, Salamone RJ, et al. CXCR4 expression in prostate cancer progenitor cells. *PLoS One* 2012;7:e31226.